REVIEW ARTICLE

Differentiation between normal skin and skin lesions using vibrational OCT

Frederick H Silver PhD[1], Ruchit G Shah PhD[2]

Silver FH, Shah RG. Differentiation between normal skin and skin lesions using vibrational OCT. J Dermatopathol. 2018;1(1):3-7.

OBJECTIVE: The need to non-invasively differentiate between skin and skin lesions has been a goal of researchers since the 1970s. While a variety of new imaging methods have been developed to evaluate the difference between normal skin and skin lesions only limited progress has been made differentiating differences in physical properties of tissues and lesions.

METHODS: We have developed a test that combines optical coherence tomography (OCT) and vibrational analysis to image and measure the moduli of the components of skin and scar tissue non-invasively and non-destructively.

RESULTS: Using images generated by OCT and measurements of the vibrational moduli, maps as a function of position can be generated that will be useful in marking the margins of scars and other skin defects. This method is calibrated by making vibrational measurements on control tissues *in vitro* and the results can be used to interpret images and measurements made *in vivo*. Results of studies on skin and scar indicate that the modulus of scar tissue *in vivo* is about 3 times that of normal skin.

DISCUSSION: Skin and skin lesions can be easily differentiated *in vivo* using vibrational OCT. This method will allow for determination of tissue margins and extent of healing of surgical and chronic skin wounds.

Key Words: *Skin, Scar, Lesion margins, Vibrational OCT, Imaging, Optical coherence tomography, Vibrational optical coherence tomography, Modulus, Mechanical properties*

The need to non-invasively and non-destructively characterize the differences between normal skin and skin lesions has been the goal of researchers for many decades. While new techniques such as phase contrast microscopy and optical coherence tomography improve image quality and resolution, these techniques do not give additional information concerning the "quality" of the extracellular matrix and changes that are associated with disease processes.

Changes in the extracellular matrix (ECM) are known to accompany the onset and progression of several highly prevalent diseases, including atherosclerosis, cirrhosis, and cancer. The relationship between cancer and tissue fibrosis has been established (1) indicating that ECM in the tumor stroma is characterized by remodeling (2). ECM stiffening has been reported to enhance cell growth and survival and promote cell migration (3) and its rigidity disrupts tissue morphogenesis by increasing cell tension (4). Increased expression of collagen is associated with elevated incidence of metastasis (5).

Optical coherence tomography (OCT) is a non-invasive, non-destructive optical technique for imaging tissue. It has been used to detect and diagnose non-melanoma skin cancer (6), visualize the functional microvasculature of the skin (7,8), evaluate the oxidative effects of hair dying (9), follow the advancement of re-epithelization of wounds (10), determine the margins of basal cell carcinomas before micrographic surgery (11), do microangiography of skin and map vascularization in plaque psoriasis (12). Quantitative uses of OCT include measurement of the surface distance to the first vessels (13), characterization of cutaneous wounds (14), thickness measurements in basal cell carcinoma and malignant melanoma (15), differentiation of benign and malignant melanoma and OCT capillaroscopy of nail folds (16).

We have developed a technique to combine OCT imaging with vibrational analysis to image and to analyze the physical properties of tissues non-invasively and non-destructively. This technique is calibrated *in vitro* using measurements made on well characterized extracellular matrices (ECMs) (17-23) and involves applying a sinusoidal sound wave to a sample at different frequencies followed by measurement of the resonant frequency of the tissue. Measurements of resonant frequency and thickness are used to calculate the elastic modulus of tissues (also termed stiffness or resistance to stretching) (20-23). For multi-component tissues such as skin, the modulus of each component can be measured simultaneously and compared to standard calibration curves for different materials. The purpose of this paper is report the use of vibrational OCT to characterize the differences between skin and scar tissue non-invasively and non-destructively based on measurement of the resonant frequencies, tissue thicknesses and elastic moduli.

METHODS

In vitro calibration curve construction using measurements on ECMs and polymers

A calibration curve of modulus values for control ECMs and Silicone rubber was constructed by comparing moduli measured using tensile testing and vibrational OCT measurements *in vitro* as previously described (17-23). The calibration curve is shown in Figure 1 and indicates a roughly one to one relationship between tensile moduli and vibrational moduli measured on the same samples including decellularized human dermis, silicone rubber and pig skin.

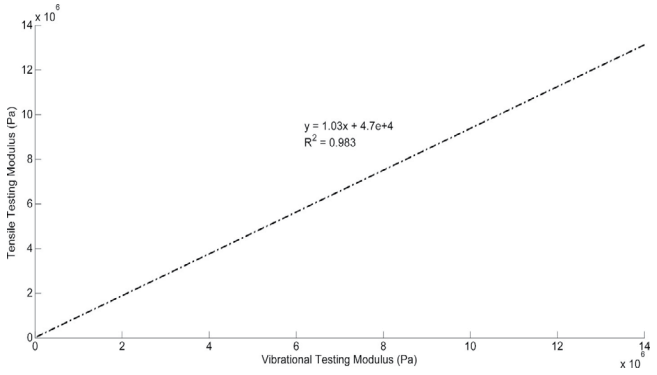

Figure 1) *Calibration curve of tensile modulus (Et) versus modulus (Ev) determined from vibrational OCT. This calibration curve was created by measuring the uniaxial tensile modulus versus strain using an incremental stress-strain experiment and calculating the vibrational modulus from resonant frequency measurements made on the same samples as reported previously. Note the almost one to one relationship between these two moduli*

[1]*Department of Pathology and Laboratory Medicine, Robert Wood Johnson Medical School, Rutgers, the State University Piscataway, NJ, 08854, USA;* [2]*Graduate Program in Biomedical Engineering, Rutgers, the State University Piscataway, NJ 08854, USA*

Correspondence: Frederick H Silver, Department of Pathology and Laboratory Medicine, Robert Wood Johnson Medical School, Rutgers, the State University Piscataway, NJ, 08854, USA. Telephone 1-732-235-4027, e-mail fhsilver@hotmail.com

Received: April 18, 2018; Accepted: April 26, 2018; Published: May 02, 2018

OPEN ACCESS

This open-access article is distributed under the terms of the Creative Commons Attribution Non-Commercial License (CC BY-NC) (http://creativecommons.org/licenses/by-nc/4.0/), which permits reuse, distribution and reproduction of the article, provided that the original work is properly cited and the reuse is restricted to noncommercial purposes. For commercial reuse, contact reprints@pulsus.com

The empirical relationship between the moduli measured using vibrational and tensile measurements was reported to be approximately linear and the equation of the line was found to be:

$$Ev = 1.026\,Et + 0.0046 \quad \text{(i)}$$

Where,

Ev and Et are the moduli measured using vibrational and tensile measurements, respectively and are in MPas. The correlation coefficient between these moduli is 0.984 as previously reported (17-20). The material behavior was reported to be reversible for strains less than about 14% for at least three cycles of tensile testing.

The resonant frequency, f_n, is related to the modulus, E, by equation (ii)

$$E = m\left(2\pi f_n\right)^2\left(\frac{L}{A}\right) \quad \text{(ii)}$$

where m, L and A are the sample mass, length and cross-sectional area. The resonant frequency was determined after correction for the resonant frequencies exhibited by the speaker and any interference due to line fluctuations (17-23). The calibration standards used are listed in Table 1.

The tensile (Et) and vibrational moduli (Ev) were obtained from references (21-26).

VIBRATIONAL OCT MEASUREMENTS

Image collection

OCT cross-sectional images were obtained using an OQ Labscope (Lumedica Inc., Durham, NC) and a laboratory spectral-domain optical coherence tomography device (SD-OCT) operating in the scanning mode (17-23).

OCT and vibrational analysis *in vivo*

Transverse sample displacement was generated by placing a speaker next to the skin and scar to be studied by spectral-domain optical coherence tomography (SD-OCT), a non-contact, interferometry technique as discussed previously. The SD-OCT system uses a fiber-coupled super luminescent diode light source with 1325 nm center wavelength and 100 nm bandwidth (full-width at half maximum) as described previously (4-6).

In vivo studies on the mechanical properties of skin and healed scar tissue were conducted by hard wiring a 24 mm × 14 mm rectangular speaker (Digi-Key, Thief River Falls, MN) to a Samsung cell phone. A frequency generating app was downloaded from the Google Play Store onto the cell phone. This app was capable of driving the speaker between 10 and 20,000 Hz. The speaker was applied to the skin using surgical tape and it was used to generate a sinusoidal sound wave that vibrated the skin. During *in vivo* measurements, no sensation of the light or sound impinging on the skin was felt. The sound intensity was low enough so that it could not be detected unless the speaker was placed near the subject's ear to make sure it was energized.

The resonant frequency of each sample was initially estimated by measuring the transverse displacement resulting from sinusoidal driving frequencies ranging from 50 Hz to 1000 Hz, in steps of 50 Hz. Once the region where the maximum frequency was identified, smaller steps of 10 Hz were used to more accurately identify the peak frequency and the actual resonant frequency, f_n. The moduli of skin and scar were calculated from measurements of the resonant frequency and tissue thickness made using vibrational OCT and images of the tissues. Moduli were obtained from a second calibration curve that relates resonant frequency to the tissue modulus times the tissue thickness (Figure 2).

The resonant frequency of skin and scar tissue were measured before and after stretching. The stretching was done by placing surgical tape above the area to be tested after deforming the tissue. The strain was approximately 50% based on the distance between two points marked on the skin before and after stretching.

TABLE 1

Calibration standards used to demonstrate relationship between tensile and vibrational moduli

Materials	Strain (%)	Cycle Number	Et (MPa)	Ev (MPa)
Decellularized Dermis	5	1	2.67	2.47
		2	2.71	2.47
		3	2.68	2.47
Pig Skin (elastic tissue)	5	1	0.87	0.75
		2	1.02	0.87
		3	0.82	0.75
Silicone Rubber	12	1	2.06	1.93
		2	1.99	1.93
		3	2.03	1.93

RESULTS

OCT images of normal scar tissue are different than that of normal skin; scar tissue appears "smoother" than the surface of normal skin (Figure 3). The plot of weighted displacement versus frequency for skin and scar tissue is shown in Figure 4 before and after stretching. Note the resonant frequency measured is only slightly dependent on the strain applied *in vivo*. The interface that separates skin and scar tissue is shown in Figure 3.

The resonant frequency values obtained from *in vivo* studies were corrected for differences in tissue thickness using the calibration curve for ECMs shown in Figure 2 to calculate values of the moduli. Plots of weighted displacement for skin and scar show peaks at 90-100 Hz (normal skin) and 220 to 230 Hz (scar tissue), respectively and the calculated moduli are about 2.0 MPa and 7.0 (scar), respectively using Figure 2 and Table 2. The values of the moduli of decellularized dermis at 5% and 15% strain are close to the values of skin and scar, respectively.

The moduli values for skin and scar as well as decellularized dermis at different strains are shown in Figure 5. From these data it appears the modulus of skin under physiologic conditions *in vivo* is about 2 MPa and is similar to the modulus of decellularized dermis at a strain of 5% *in vitro*. The modulus of scar is about 7 MPa *in vivo* and is similar to the modulus of decellularized dermis at a strain of about 15% *in vitro*.

Figure 6 shows a stress-strain curve for human decellularized dermis measured *in vitro* showing the low and high modulus regions characteristic of the mechanical behavior of skin. Note that normal

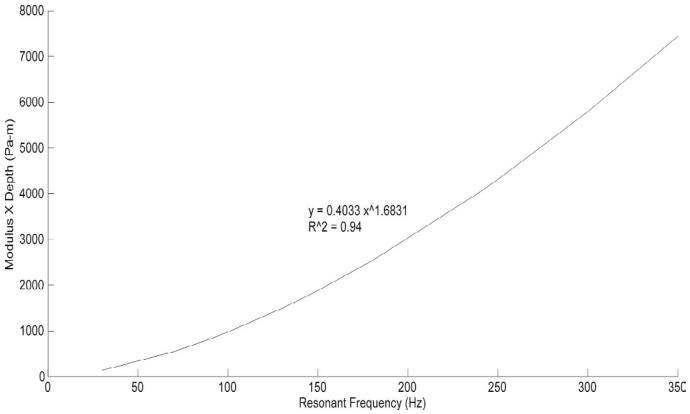

Figure 2) *Calibration curve of elastic modulus times sample thickness versus resonant frequency for different extracellular matrices. The modulus values were calculated from tensile measurements and the resonant frequency from vibrational measurements. Note the elastic modulus of decellularized dermis increases with strain*

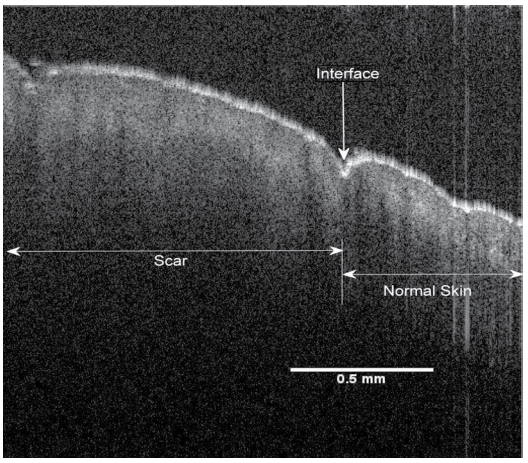

Figure 3) *OCT images of skin and scar. These images were produced using a Lumedica OQ Labscope operating in the scanning mode. Note the difference in surface texture of normal skin and scar tissues*

TABLE 2

Calculated vibrational moduli for skin, scar and decellularized dermis. These moduli were calculated from experimental values of the resonant frequency and tissue thickness using Figure 2. Based on the vibrational data on decellularized dermis the strain *in vivo* for skin is about 5%

Materials	Strain (%)	Thickness (mm)	Resonant Frequency (Hz)	Modulus (MPa)
	5		150	2.48
Decellularized Dermis	10	1.2	180	4.88
	15		250	6.82
Pig Skin (Elastic)	5	3	90	0.75
Pig Skin (Collagen)	5	3	200	3.55
Human Skin (*in vivo*)	5	0.46	100	2.12
Human Scar (*in vivo*)	5	0.54	220	6.49

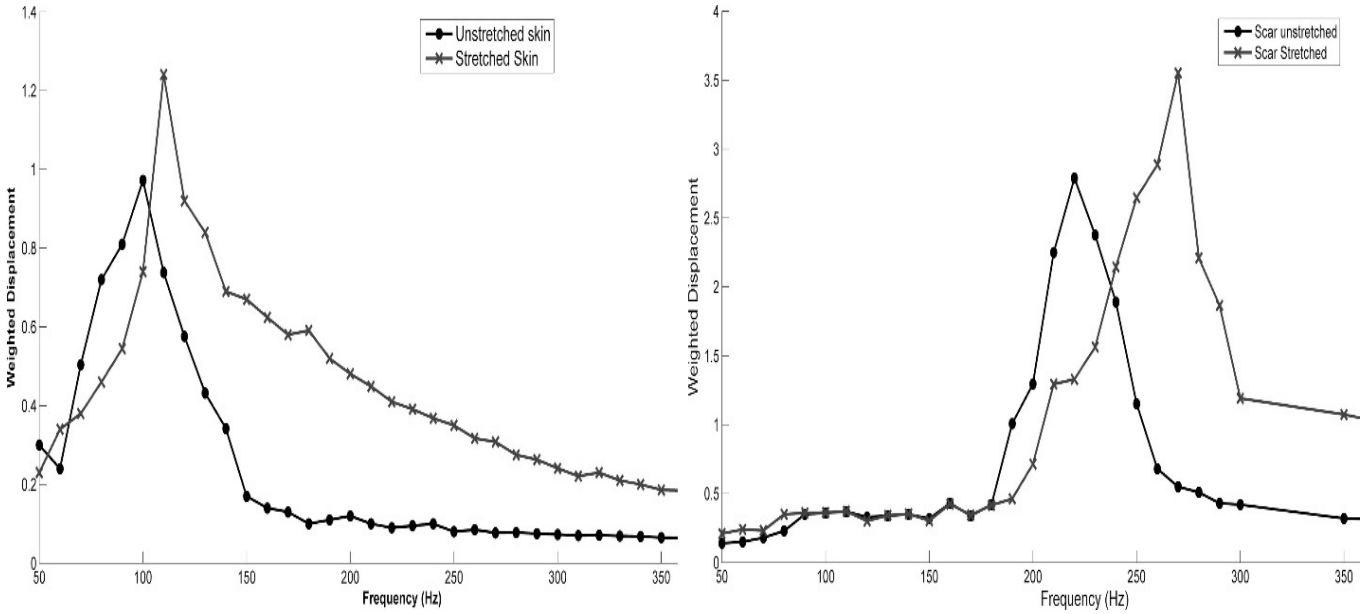

Figure 4) *Weighted displacement versus frequency for unstretched and stretched normal skin (left) and unstretched and stretched scar (right). The amount of stretch was approximately 50% based on measurement of the distance between two points before after stretching.*

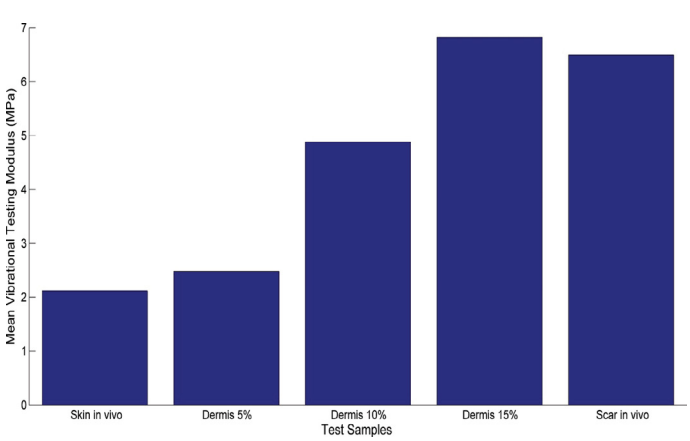

Figure 5) *Bar graph comparing vibrational moduli values measured for decellularized human dermis at 5%, 10% and 15% strain in vitro and skin and scar in vivo. Note the values of vibrational moduli for skin and scar in vivo are similar to the moduli for decellularized dermis at 5% and 15 %, respectively. The higher modulus for scar tissue appears to be a result of the more random orientation of the collagen fibers and the inability of the fibers to reorient along the stress direction when a load is applied*

skin is operating in the low modulus region while scar operates in the high modulus region.

DISCUSSION

Recently, we have reported the use of vibrational analysis and OCT to characterize the mechanical behavior of decellularized dermis, pig skin;

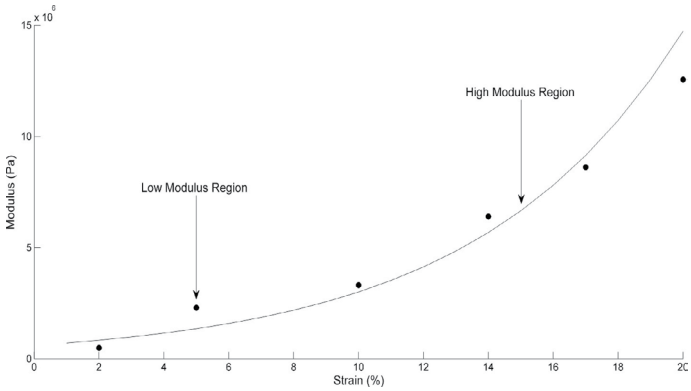

Figure 6) *Vibrational modulus versus strain curve for human decellularized dermis. This curve is characteristic of the mechanical behavior of skin and other collagenous tissues. Note normal skin is operating in the low modulus region (modulus about 2 MPa) while scar operates in the high modulus region (modulus of 7 MPa)*

bovine cartilage and subchondral bone *in vitro* and human skin and scar *in vivo*. In this paper we report a method to convert resonant frequency and thickness measurements on skin and scar tissues *in vivo* into calculated values of the moduli. In addition, we discuss the physical differences between normal skin and scar based calculated modulus measurements and OCT images.

The ability to measure the mechanical properties of skin and skin lesions *in vivo* non-invasively and non-destructively has been a challenge to the biophysical scientist since the 1970s. The pioneering work of Yamada

(24) and Fung (25) illustrated how difficult this goal would be since the behavior of human ECM depends on strain-rate, direction of testing and is time-dependent (26). A variety of methods have been used to evaluate the mechanical properties of skin over the last 40 years including uniaxial and biaxial tensile testing, indentation and rotational tests, ultrasound elastography (UE), optical coherence tomography (OCT), optical coherence elastography (OCE), and vibrational analysis combined with OCT. Many of these techniques require the assumptions that the material is linearly elastic, Poisson's ratio is close to 0.5 (deformation at constant volume) and that viscoelasticity does not dramatically affect the resulting properties of the tissue. However, skin is a non-linear material that is viscoelastic and has upward curvature to the stress-strain curve. This fact makes determination of the stiffness (tangent to the stress-strain curve) and other mechanical properties very difficult to quantitatively analyze since the tangent to the stress-strain curve is constantly changing. However, despite all of these problems, there is a need to be able to characterize the mechanical properties of skin, since this would give clinicians valuable information about changes that occur during disease processes, the stage of diabetic skin ulcers and the efficacy of cosmetic treatments. This paper describes the use of vibrational OCT to image and to determine the physical characteristics of skin and scar tissues.

By calculating the modulus at the resonant frequency it is possible to eliminate the viscous contribution to the mechanical properties. By pulsing tissues with a series of sinusoidal sound waves as a function of the frequency, the viscous contribution can be shown to almost disappear at the resonant frequency. The viscous contribution of skin has been shown to as high as 25% at low strains and strain-rates and as low as 3% to 4% at high strains and strain-rates. However, measurements made at the resonant frequency simplify the analysis since they are independent of strain-rate.

Vibrational OCT is based on the observation that when tissues are vibrated at their resonant frequencies they undergo maximum displacement which can be measured by OCT. The resonant frequency of a material is related to the sample dimensions and the elastic modulus.

Previous studies of skin and hypertrophic scar suggest that the modulus values determined using tensile stress-strain measurements for normal skin and scar are similar and only the ability to deform these tissues were found to be different (27). In this study we report that scar was at least three times stiffer than normal skin under physiological conditions.

While the results in this study appear to contradict previous reports, on closer examination they underscore the utility of vibrational OCT to define structural and mechanical differences that can be observed using this technique. In the previous study the modulus measurements were made from the slope of tensile stress-strain curves which require drawing a tangent to the stress-strain curve. To make modulus measurements from stress-strain curves requires curve fitting techniques and measurements of several stress and strain points. Thus the modulus at any one strain cannot be determined and can only be approximated for certain strain regions such as for low and high strain regions (Figure 6).

In contrast, using vibrational OCT modulus measurements can be made at any strain at a single point. This allows one to compare neighboring regions of normal skin and scar making only a single measurement at each location. Furthermore using surgical tape to stretch the skin the modulus at several strains can be measured. The ability to relate *in vivo* measurements to calibration curves (Figures 1 and 2) provides standards against which to compare the experimental measurements.

The results presented in this paper suggest that skin and scar have different OCT images and moduli. The significance of these measurements lies in the ability to discern differences in the structures of these tissues. While normal skin contains a planar almost biaxial arrangement of collagen fibers that provide mechanical reinforcement to the skin preventing premature mechanical failure scar tissue is more randomly organized and cannot rearrange as easily under tensile mechanical loads.

It is well known that mature scar tissue never reaches the mechanical strength of normal skin after wound healing is completed (28). However, scar tissue "appears" stiffer to the touch because it operates at an "effective" higher net strain due to its inability to undergo deformation. This observation indicates that scar tissue under physiologic conditions operates in the high modulus region as illustrated in Figure 6. Scar tissue appears to operate at a higher stress under physiological conditions and may explain why it tears more easily than normal skin.

CONCLUSION

Using vibrational OCT, the resonant frequency and moduli of the components of skin and scar tissue can be measured non-invasively and non-destructively. The numbers generated reflect to a first approximation the elastic moduli and do not depend on measurement of other parameters. The technique is calibrated *in vitro* using incremental tensile stress-strain measurements and vibrational OCT tests on the same sample. Using images generated by OCT, maps of the modulus as a function of position can be generated that will be useful in marking the margins of skin and skin lesions. Differences in the moduli of skin and skin lesions can be interpreted based on OCT images and an understanding of the relationship between tissue macromolecular content, the collagen orientation and mechanical properties of ECMs.

REFERENCES

1. Leventhal KR, Yu H, Kass L, et al. Matrix crosslinking forces tumor progression by enhancing integrin signaling. Cell. 2009;139:891-06.
2. Butcher DT, Allston T, Weaver VM. A tense situation: Forcing tumor progression. Nat Rev Cancer. 2009;9:108-22.
3. Lo GM, Wang HB, Dembo M, et al. Cell movement is guided by the rigidity of the substrate. J Biophys. 2000;79:144-52.
4. Paszek MJ, Zahir N, Johnson KR, et al. Tensional homeostasis and the malignant phenotype. Cancer Cell. 2005;8:241-54.
5. Ramaswamy S, Ross KN, Lander ES, et al. A molecular signature of metastasis in primary solid tumors. Nat Genet. 2003;33:49-54.
6. Gambichler T, Regeniter P, Bechara FG, et al. Characterization of benign and malignant melanocytic skin lesions using optical coherence tomography *in vivo*. J Am Acad Dermatol. 2007;57:629-37.
7. Baran U, Choi WJ, Wang RK. Potential use of OCT-based microangiography in clinical dermatology. Skin Res Technol. 2016;22: 238-46.
8. Baran U, Swanson E, Sanders JE, et al. OCT-based microangiography for reactive hyperaemia assessment within residual limb skin of people with lower limb loss. Skin Res Technol. 2018;24:152-5.
9. Robles MVR, Zanardi A. Optical coherence tomography to evaluate the effects of oxidative hair dye on the fiber. Skin Res Technol. 2016;22:430-4.
10. Ahlstrom MG, Gjerdrum LMR, Larsen HF, et al. Suction blister lesions and epithelialization monitored by optical coherence tomography. Skin Res Technol. 2018;24:65-72.
11. Schuh S, Kindermann N, Kästle R, et al. Optical coherence tomography for margin definition of basal cell carcinoma before micrographic surgery recommendations regarding the marking and scanning technique. Skin Res Technol. 2018;24:145-51.
12. Odorici G, Losi A, Ciardo S, et al. Non-invasive evaluation of Secukinumab efficacy in severe plaque psoriasis with confocal microscopy and optical tomography: A case report. Skin Res Technol. 2018;24:160-2.
13. Sigsgaard V, Themstrup L, Theut RP, et al. *In vivo* measurements of blood vessels distribution in non-melanoma skin cancer by dynamic optical coherence tomography: A new quantitative measure. Skin Res Technol. 2018;24:123-8.
14. Kuck M, Strese H, Arash Alawi S, et al. Evaluation of optical coherence tomography as a non-invasive diagnostic tool in cutaneous wound healing. Skin Res Technol. 2014;20:1-7.
15. Mogensen M, Nurnberg BM, Forman JL, et al. *In vivo* thickness measurement of basal cell carcinoma and actinic keratosis with optical coherence tomography and 20 MHz ultrasound. Br J Dermatol. 2009;160:1026-33.
16. Ring HC, Themstrup L, Alette Banzhaf C, et al. Dynamic optical coherence tomography capillaroscopy a new imaging tool in autoimmune connective tissue disease. JAMA Dermatol. 2016;152:1142-6.
17. Shah RG, Silver FH. Vibrational analysis of extracellular matrix scaffolds: Comparison of skin, dermis, cartilage and subchondral bone. Adv Tissue Eng Regen Med. 2017;2:48.
18. Silver FH, Shah R. Measurement of mechanical properties of natural and engineered implants. Adv Tissue Eng Regen Med. 2016;1:1-9.

19. Silver FH, Silver LL. Non-invasive viscoelastic behavior of human skin and decellularized dermis using vibrational OCT. Derm Clin Res. 2017;3:174-9.

20. Shah R, DeVore D, Pierce MG. Morphomechanics of dermis-A method for non-destructive testing of collagenous tissues. Skin Res Tech. 2016.

21. Shah R, Pierce MC, Silver FH. A method for non-destructive mechanical testing of tissues and implants. J Biomed Mat Res. 2017;105:5-22.

22. DeVore D, Silver FH. Biomechanical analysis of de-cellularized dermis and skin: Initial *in vivo* observations using OCT and vibrational analysis. J Biomed Mat Res. 2018.

23. Shah RG, Silver FH. Viscoelastic behavior of tissues and implant materials: Estimation of the elastic and viscous contribution using optical coherence tomography and vibrational analysis. J Biomed Tech Res. 2017;3:105.

24. Yamada H, Evans FG. Strength of biological materials. University of Michigan. 1970.

25. Fung YC. Biomechanics: Mechanical properties of living tissue. Springer. 1973.

26. Dunn MG, Silver FH. Viscoelastic behavior of human connective tissues: Relative contribution of viscous and elastic components. Connect Tissue Res. 1983;12:59-70.

27. Silver FH, Swann DA. Mechanical analysis of hypertrophic scar tissue: Structural basis for apparent increased rigidity. J Invest Dermatol. 1985;84:9-13.

28. Doillon CJ, Dunn MG, Bender E, et al. Collagen fiber formation in repair tissue: Development of strength and toughness. Collagen Res ReI. 1985;5:481-92.